Environmental Earth Sciences (2023) 82:72
https://doi.org/10.1007/s12665-023-10751-3

ORIGINAL PAPER

Retention potential of a drained wetland in the Lusatian lignite mining district, Briesener Niedermoor, Germany, Europe

Clemens Hartmann[1] · Wilfried Uhlmann[2] · Traugott Scheytt[1]

Received: 11 October 2022 / Accepted: 8 January 2023 / Published online: 20 January 2023

Abstract
Acid mine drainage (AMD) is one of the most important global causes for polluted water. It occurs in mining areas due to oxidation of sulfide minerals. Depending on hydrological conditions, wetlands are considered suitable for passive treatment of AMD. The aim of the study was to characterize the long-term retention performance of a drained wetland, Briesener Niedermoor, in an iron and sulfate contaminated catchment area. The site is located in the Lusatian lignite mining district, Germany. Hydrological and hydrochemical measurements as well as time series of groundwater and surface water were evaluated and saturation conditions of iron species were determined using Phreeqc Interactive and E_H–pH diagrams for the Fe–S–K–O–H system. Progressing peat degradation due to drainage leads to a hydraulic behaviour of the wetland that is more comparable to a rain bog than a fen, and thus to more pronounced oxic conditions. Groundwater feeds the wetland with significant loads of iron and sulfate, which are temporally stored in the wetland. At low surface water discharge, iron is removed and weak acidic pH is buffered by the dominant phase of schwertmannite ($Fe_8O_8(OH)_6SO_4$), usually during summer months. In winter, greater water availability initializes a high source strength from the wetland, that cannot be retarded. Thus, only during summer, there is a retention potential; in winter, the retention potential is not strong enough to prevent an inflow of iron and sulfate. Only a significant rewetting of the wetland may result in a restoration of the retention potential of the wetland Briesener Niedermoor.

Keywords Iron · Sulfate · Drained wetland · Time series · Groundwater · Surface water

Introduction

Acid rock drainage (ARD) is formed by oxidation of metal sulfides, commonly pyrite and pyrrhotite, when exposed to natural water and oxygen. This results in the release of iron, aluminium, sulfate, toxic metals, trace elements, and acid in water (Blowes et al. 2014; Carrero et al. 2015). Further oxidation of ferrous iron, subsequent hydrolysis, and precipitation of ferric oxy(hydroxides) and hydroxysulfates lead to additional acidity (Nordstrom et al. 2015). Because these processes are mainly attributed to active and abandoned mining sites of coal and sulfide ore, the term acid mine drainage (AMD) is commonly used, being one of the current global environmental issues (Wolkersdorfer and Bowell 2004; Tutu et al. 2008; Galhardi and Bonotto 2016).

Although the chemistry of AMD generation by sulfide–mineral oxidation is well known (Nordstrom 1982), the processes are complex in detail. Great importance is attached to the oxidation of ferrous iron to ferric iron, mainly mediated by microbial activity at low pH values (Küsel 2003), because ferric iron is a more effective oxidant than oxygen (Nordstrom et al. 2015). The oxidation rates are mainly affected by pH, the presence of microorganisms, dissolved ferric iron concentration, temperature (T), redox potential (E_H), and dissolved oxygen concentration (O_2) (Blowes et al. 2014) that have been the focus of previous study (Wiersma and Rimstidt 1983; Moses et al. 1987; Sasaki 1994; Dos Santos et al. 2016). In the absence of oxygen ferrous iron dominates, such in groundwater, the iron oxidation is more complex under atmospheric conditions: varying hydrological and meteorological impacts

✉ Clemens Hartmann
Clemens.Hartmann@geo.tu-freiberg.de

[1] Institute of Geology, Department for Hydrogeology and Hydrochemistry, Technical University Bergakademie Freiberg, Gustav-Zeuner-Straße 12, 09599 Freiberg, Germany

[2] Institut für Wasser und Boden Dr. Uhlmann, Lungkwitzer Straße 12, 01259 Dresden, Germany

(Nordstrom 2009; Uhlmann et al. 2013; Kruspe et al. 2014) and hydro(bio)chemical self-propagation as well as self-regulation factors (Bigham et al. 1990; Peine et al. 2000; Regenspurg 2002; Küsel 2003) change pH conditions, microbial activity, oxidation states, and dissolved iron concentrations and thus the mobility of iron and other metals.

AMD results in decreasing water quality and sedimentation of toxic metals and thus in negative effects on aquatic ecology. AMD characteristics are already described in detail in various studies around the world, such as in Brazil (Galhardi and Bonotto 2016), in the Iberian Pyrite Belt, Portugal and Spain (Sáinz et al. 2002; Moreno-González et al. 2022), and in the Lusatian coal mining district, Germany (Uhlmann et al. 2010, 2013). Because it poses a risk for environmental damage in the surface and subsurface catchment areas, strategies are needed to attenuate AMD.

Numerous treatment technologies have been evaluated including chemical and passive systems (Skousen et al. 2000, 2017; Ighalo et al. 2022). Because passive treatment technologies provide an ecological, less cost-intensive and low-maintenance alternative (Moreno-Mateos and Comin 2010), they are gaining more attention in research. Passive systems include the so-called constructed wetlands and natural wetlands (Skousen et al. 2017). Wetlands are considered to have a long-term potential for remediation of AMD species (August et al. 2002), improvement of water quality downstream (Sasaki et al. 2001; August et al. 2002; Dean et al. 2013; McCarthy et al. 2016), and hydraulic buffering (Lamers et al. 2015). Depending on hydrology, different beneficial physical, chemical, and biological properties of the wetlands allow settling, sedimentation, sorption, co-precipitation, cation-exchange, photodegradation, phytoaccumulation, biodegradation, microbial activity, plant uptake, and thereby removal of AMD species (Sheoran and Sheoran 2006). The objective of this research is to study these natural processes in constructed wetlands (Sheridan et al. 2013; Pat-Espadas et al. 2018; Sekarjannah et al. 2019; Zubair et al. 2020; Messer et al. 2021). Although natural wetlands cover 3% of the global land area (Lamers et al. 2015), they are not studied as intensively as constructed wetlands as a potential treatment of AMD (Bayley et al. 1986; Beining and Otte 1996; Sasaki et al. 2001; August et al. 2002; Dean et al. 2013).

Whether a wetland acts as a sink or source depends highly on hydrological conditions (Devito and Hill 1997; Eimers et al. 2008), that can be changed long term and seasonally (August et al. 2002). The hydrological conditions determine the residence time, AMD load, and whether aerobic or anaerobic conditions are established in the wetland. While anaerobic conditions cause the removal of sulfate and metals by precipitation of metal sulfides (Humphries et al. 2017) by sulfate reducing bacteria (Dean et al. 2013) and subordinately of (oxy)hydroxides and carbonates, aerobic conditions result mainly in precipitation of metal (oxy)hydroxides (Skousen et al. 2000). In iron-sulfate dominated environments, especially acid iron and aluminium hydroxysulfates such as schwertmannite can act as important host phases for sulfate and metals (Bigham et al. 1996; Schöpke 2007; Carrero et al. 2015; Burton et al. 2021), whose dominance has been already observed in surface waters in Lusatia (Uhlmann et al. 2010).

Lusatia, located in South Brandenburg and Northeast Saxony, is one of the largest lignite mining areas of Germany, Europe and rich in wetlands that currently cover an area of 2100 km^2 in Brandenburg (Landgraf 2010). Since mining became industrial in the middle of the nineteenth century, long-term intervention in the regional water balance has caused strong effects on redox conditions and hydraulic conditions. Due to mining-induced groundwater drawdown and subsequent flooding of post-mining lakes, AMD has been generated and is locally associated with natural wetlands. Sources of AMD, mainly characterized by high sulfate and iron concentrations in groundwater and surface water, are located in Pleistocene aquifers and Holocene wetlands, being rich in sulfide minerals due to anoxic formation conditions (Kruspe et al. 2014). Local significant amounts of bog iron ore in wetland peats (Uhlmann et al. 2010; Kruspe et al. 2014) are also potential iron sources. 75% of the wetlands are currently used for agriculture in Brandenburg (Landgraf 2010) and thus degraded, resulting in changed peat structure and hydrological conditions.

However, wetlands significant but sensitive function in retention is well known and it has been identified as one of the potential sources of iron and sulfate in Lusatia. No attention has been paid to determine the current role in retention of AMD species by a long-term hydrologically changed wetland. There is only a poor understanding of the performance of these drained and degraded wetlands over a long time period in hydrology, matter supply, storage, transformation, and output. The study aims to identify the source, main flow paths, and transformation processes of iron and sulfate in the Briesener Wiesengraben in Lusatia, Germany and subsequently decide whether this local wetland can protect the surface water from AMD.

Materials and methods

Study site

The 11.5 km^2 investigation area is located in the northern region of the Lusatian lignite mining district, 100 km south of Berlin, 90 km north of Dresden, Germany, Europe (Fig. 1). It includes the surface and subsurface catchment area of the river Briesener Wiesengraben,

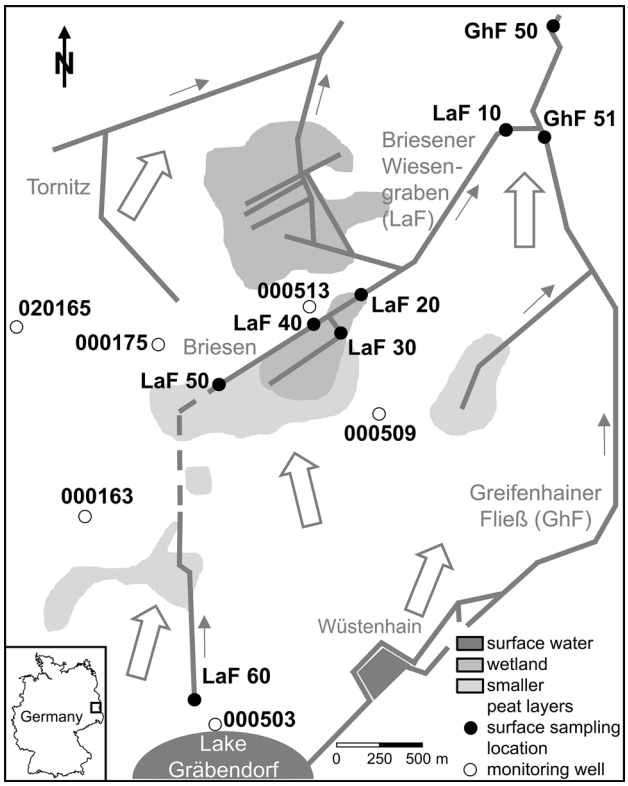

Fig. 1 Simplified map of the investigation area with located surface water bodies, wetlands, sampling points, and regional groundwater flow direction (empty arrows, based on LMBV mbH 2019)

former Laasower Fließ (LaF), draining a natural wetland (4 km^2) and flowing into Greifenhainer Fließ (GhF). The morphology originates from Pleistocene fluviatil and limnic valley and basin fills, slope sands and debris cones (Landesvermessung und Geobasisinformation Brandenburg 2022). The investigated porous aquifer is streaked by silt and clay and covered by Holocene layers, including fens with surrounding smaller peat layers in the lowlands (Landesvermessung und Geobasisinformation Brandenburg 2022). Because of local groundwater drawdown through peat mining and agricultural use and regional groundwater drawdown due to coal mining, the peat has a maximal thickness of 55 cm (Uhlmann et al. 2010). The corrected average long-term annual precipitation between 1981 and 2010 is 625 mm (Deutscher Wetterdienst 2021). The climatic water balance is characterized by strongly water-deficient summer months with weeks to months of prolonged hot and dry periods (Krümmelbein et al. 2012) and water surplus winter months, causing annual water deficits from 2010/2011 to 2018/2019 (Deutscher Wetterdienst 2021). The dominating land use of the wetland is live-stock farming, whereas the surrounded area is forested and agricultural.

Sample collection and analyses

Measurements were carried out for surface water and groundwater in summer 2019: on-site parameters have been determined, water samples were collected, and the groundwater table was measured. Three sampling locations were measured in surface water (LaF 50, LaF 40, and LaF 20). The discharge rate of the drainage stream was measured by magnetic-inductive flow meter OTT Hydromet OTT MF. Groundwater was sampled at five location sites in the catchment area of the wetland (000163, 000175, 000503, 000509, and 000513). 020165 was investigated to characterize groundwater that is potentially hydrochemically unaffected by both Lake Gräbendorf and the wetland.

pH, E_H, electrical conductivity (EC), T, and O_2 were determined by electrodes of HACH HQ40D Digital two-channel multi-meter at each sampling location on-site. Total and carbonate hardness were titrimetrically measured using Merck MColortest™ in the field. All samples were stored cool in airtight tubes and dark conditions until analysis in the laboratory. The concentrations of the iron species were photometrically determined by HACH DR/890 colorimeter, whereby total iron and total dissolved iron concentration were measured by Ferro-Ver-method and ferrous iron concentration by 1,10-Phenanthrolin-method. The ferric iron concentration was determined by difference measuring of total dissolved iron and ferrous iron concentration. Main anions and cations were measured by conductivity detector of Metrohm liquid ion chromatograph 881 Compact IC pro as well as dissolved organic carbon (DOC) by NDIR detector of Analytik Jena multi-N/C 2001 S analyser.

Data processing

A groundwater plan was modelled by Processing Modflow (Chiang and Kinzelbach 2001). Geochemical equilibrium calculations were performed by Phreeqc Interactive (USGS 2020). Therefore, two models with different input parameters were used based on own measured data and the database phreec.dat of Phreeqc Interactive (USGS 2020), added by the mineral phase schwertmannite with log $K = 18$ (Bigham et al. 1996). The data of reference measurements were extended by pre-existing long-term monitoring data (LMBV mbH 2019), such as groundwater table, discharge rate, pH, E_H, concentration of different iron species, and acid and base capacity. For this purpose, data were available for all sampling points of LaF, 2 of GhF and 2 of groundwater (000503, 000509) from 2007 to 2019. Data of 000503, 000509, 000513, 000163, and

000175 were accessible for long-term observing groundwater table.

Pyrite oxidation, hydrolysis, and acidification

AMD is initialized in both oxic and anoxic systems through geochemical, microbiological, or electrochemical pathways by oxidation of metal sulfide minerals when their surfaces are exposed to water and an oxidant, including oxygen, ferric iron, or mineral catalysts (Nordstrom et al. 2015). Using the example of pyrite oxidation by atmospheric oxygen, ferrous iron is produced (Eq. 1) that can be oxidized to ferric iron by acidophilic lithoautotrophic bacteria (Küsel 2003) under acid conditions (Eq. 2, Bigham et al. 1990). Microbial activity is a key driver in accelerating ferric iron production and pyrite oxidation. If ferric iron is present in solution, mainly at pH values under 4 (Berghorn and Hunzeker 2001), it acts as a major oxidant and accelerates the pyrite oxidation in a self-propagating cycle (Eq. 3, Bigham et al. 1990; Küsel 2003). In most AMD samples, ferrous iron is dominant, indicating a faster oxidation of sulfide minerals than of ferrous iron.

$$FeS_2 + \frac{7}{2}\,O_2 + H_2O \rightarrow Fe^{2+} + 2\,H^+ + 2\,SO_4^{2-} \quad (1)$$

$$Fe^{2+} + \frac{1}{4}\,O_2 + H^+ \rightarrow Fe^{3+} + \frac{1}{2}\,H_2O \quad (2)$$

$$FeS_2 + 14Fe^{3+} + 8\,H_2O \rightarrow 15\,Fe^{2+} + 16\,H^+ + 2\,SO_4^{2-}. \quad (3)$$

By reacting with water, ferric iron is stepwise hydrolysed after a delay that leads to the formation of ferric iron minerals and pH reduction (Eq. 4). Due to their low solubility (Schwertmann 1991), schwertmannite, goethite, ferrihydrite, and jarosite usually precipitate as mixtures in the surface waters according to their different stability fields (Bigham et al. 1996; Nordstrom et al. 2015). Which mineral phase predominates depends on pH and sulfate activity, among others (Bigham et al. 1994). In the case of ferrihydrite, it precipitates at neutral pH conditions and low sulfate activity (Eq. 5).

$$Fe^{3+} + 3\,H_2O \rightarrow Fe(OH)_3 + 3\,H^+ \quad (4)$$

$$Fe(OH)_3 \rightarrow Fe(OH)_3(s). \quad (5)$$

The simplified overall reaction of Eq. 1, Eq. 2, Eq. 4, and Eq. 5 for ferrihydrite can be written as (Eq. 6)

$$4\,FeS_2 + 15\,O_2 + 14\,H_2O \rightarrow 16\,H^+ + 8\,SO_4^{2-} + 4Fe(OH)_3(s). \quad (6)$$

The acidity thus produced can be buffered by the natural background alkalinity leading to higher pH values and thus to the formation of ferric iron precipitates. Once the alkalinity is depleted, surface waters acidify and the solubility of metals, especially ferric iron, increases. This can restart the cycle of pyrite oxidation until pyrite and ferric iron are consumed. Various studies showed that schwertmannite is the dominant ferric mineral phase under pH conditions between 2.5 and 4 (Bigham et al. 1990) and controls the pH conditions significantly and thus both the major- and trace-element mobility in surface waters (Bigham et al. 1990, 1994; Regenspurg 2002; Küsel 2003; Knorr and Blodau 2007). As long as a constant ferrous iron supply and oxidation are observed, no change of the acid pH conditions is expected (Bigham et al. 1990; Regenspurg 2002) and hydrolysis and precipitation continue in surface water. Besides these chemical reactions for AMD generation, the concentrations of metals, acid, and their loadings are also influenced by seasonal variations of precipitation infiltration rates (Nordstrom 2009).

Results

Reference measurements

At the measuring time, the wetland's surface was dry, and the drainage stream carried only water between LaF 50 and LaF 20 without any discharge rate, characterized by yellowish-orange colour, high turbidity, and macroscopically visible iron and organic particles. The riverbed and the shore were sedimented by local iron mineral layers with a thickness of up to a few cm.

The pH of the drainage stream, being iron-sulfate dominated, is neutral and it does not change downstream in contrast to the increasing weak E_H, the low O_2, and the high turbidity (Table 1). On the other hand, the acid capacity up to pH 4.3 decreases dramatically from LaF 50 to LaF 20. Sulfate, the dominant nitrogen species ammonium, and DOC increase downstream while passing the wetland, confirmed by maximal concentrations and maximal EC in LaF 40. The concentrations of total iron occur predominantly as ferrous iron, whereby the acidic and oxidative water of the downstream (GhF) shows pronounced ferric iron concentrations. Large local dependencies in redox conditions and ion concentrations in groundwater were observed. The acid capacity up to pH 4.3, pH, and O_2 of the groundwater northwest of the wetland (000175) are similar to LaF 50. The eastern groundwater (000509, 000513) is neutral to weakly acidic, weakly buffered, and more oxidizing. The groundwater north of the wetland (000513) stands out with high total dissolved

Table 1 Reference measurements of hydrochemical standard parameters and main ions

Site		Groundwater			Surface water			
		000509	000513	000175	Drainage stream			Downstream
					LaF 50	LaF 40	LaF 20	GhF50
T	[°C]	11.2	12.4	11.6	19.1	22.1	23.2	21.7
pH	[]	4.7	5.1	6.6	7.1	6.5	6.6	3.0
E_H	UH, 25 °C [mV]	305	245	127	88	134	204	645
O_2	[mg/L]	0.2	1.0	1.1	0.8	1.0	1.0	4.2
Alkalinity	[mmol/L]	0.4	0.9	8.0	6.8	3.6	1.5	o. d. l.[a]
Turbidity	[FNU]	9.3	62.2	1.5	243	279	408	5.3
EC	[µS/cm]	1060	2140	2850	2040	2140	2040	1440
Ferrous iron Fe^{2+}	[mg/L]	156	248	113	94	204	167	22
Ferric iron Fe^{3+}	[mg/L]	0	21	2	2	14	3	12
Total iron	[mg/L]	284	> 300	> 300	109		191	30
SO_4^{2-}	[mg/L]	660	1360	1720	940	1400	1460	960
NO_3^-	[mg/L]	< 0.1	< 0.1	< 0.1	0.3	2.3	0.3	0.2
NH_4^+	[mg/L]	1.5	4.9	1.4	2.5	4.5	4.7	1.6
DOC	[mg/L]	6.1	40.1	3.9	36.0	56.2	40.7	6.2

[a]Out of detection limit

iron, sulfate, ammonium, and DOC concentrations, comparable to surface water near the wetland.

Phreeqc Interactive (USGS 2020) showed that the ferric iron concentration is generally overestimated by the measuring method, confirmed by modelled small ferric iron concentrations and redox potentials (Online Resource 1). The controlling ferric iron mineral phase of the surface water except from the downstream is schwertmannite, but goethite, ferrihydrite, and locally K-jarosite are also oversaturated. While the saturation indices of the iron minerals increase downstream in the drainage stream, the surface water shows minimal saturation indexes of iron minerals at maximal iron concentrations in the wetland. The saturation indices of siderite and calcite decrease with reducing acid capacities up to pH 4.3 downstream.

Hydraulics

The groundwater table is nearly constant with fluctuations of 1 m in the investigation area since 2007, while the depth to groundwater weakly varies between 2.0 and 2.5 m in the east and 2.5 m and 4 m in the west. According to the measured groundwater tables, the groundwater flows northwards from Lake Gräbendorf to the wetland, being fully confined by groundwater, and potentially infiltrating into surface water from LaF 50 to LaF 20. However, the modelled groundwater plan shows that the hydraulic connection between wetland and groundwater is inhibited. The fact that no baseflow is temporally observed in summer confirms this assumption. Schmidt (2013) observed similar characteristics on surrounding wetlands. In contrast to summer, water is temporally logging on wetland's surface in winter. From LaF 20 downstream, there is infiltration induced by the lower groundwater table and shown by decreasing discharge rates.

With respect to the time series of the discharge rates and discharge rate balances, the surface water gains the nearly most input from the wetland. While it carries negligible amounts at LaF 50, the discharge rate is higher in the area of the wetland with respective average rates of up to 0.006 m^3/s. Downstream the discharge rate balance between LaF 10 and the sum of LaF 30 and LaF 40 is negative, indicating infiltration. From 2009 to 2019, the discharge rate correlates with the seasonal variation of the climatic water balance and thus of the available precipitation infiltration supply. It results in low discharge rates in summer, that even tend to 0 m^3/s, and maximal discharge rates up to 0.05 m^3/s in winter, especially in the downstream of the drainage stream.

Time series of hydrochemical data

Between 2009 and 2019, long-term constant pH values from 4 to 6 and low acid capacities up to pH 4.3 are observed in groundwater. The upper stream, including the passage through the wetland, is dominated by pH values from 6 to 7 and acid capacities up to pH 4.3 from 2 to 6 mmol/l (Fig. 2, Online Resource 2), that are similar to proximal groundwater in 000175 at the measuring date. After passing the wetland, the hydrochemistry of the surface water changes significantly by formation of two plateaus: While pH values from 5.5 to 6.5 with simultaneous acid capacities up to pH 4.3 up to 2 mmol/L mainly occur in winter, pH values from

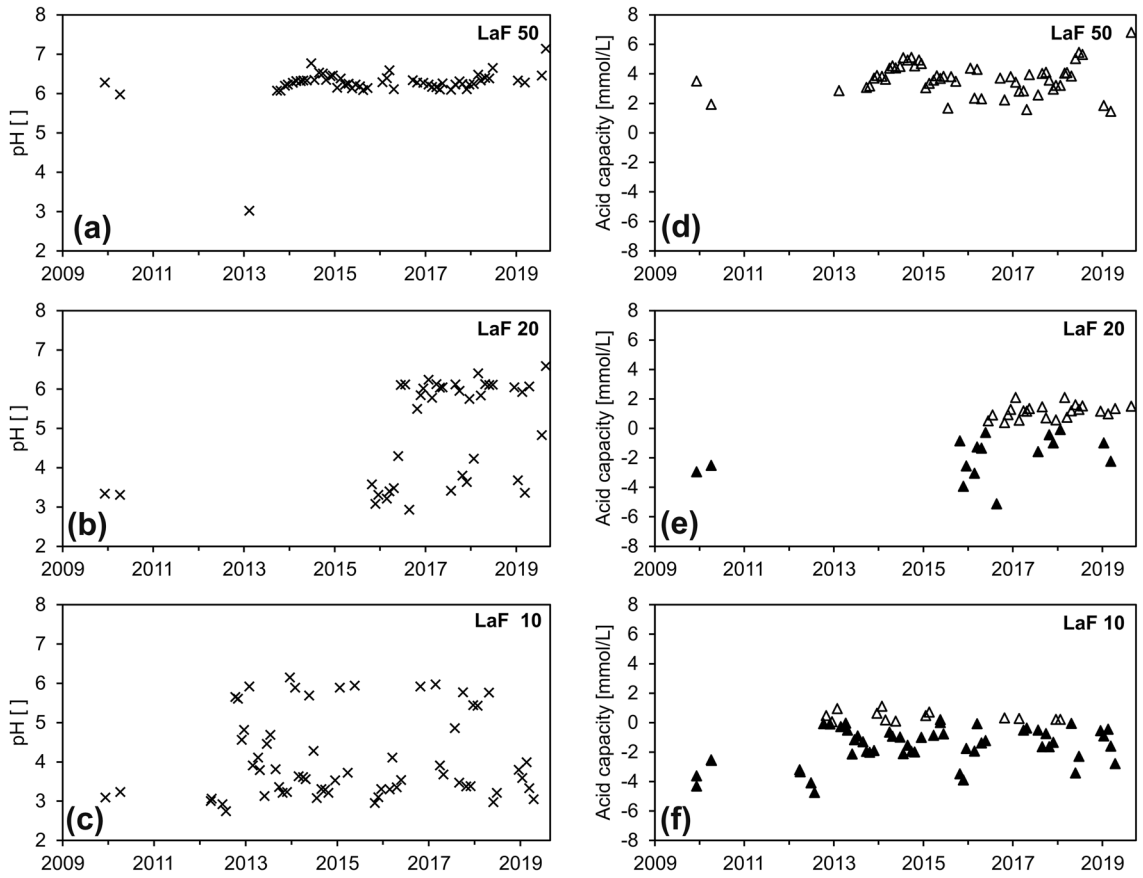

Fig. 2 Time series of pH values (**a**, **b**, **c**) and acid capacity up to pH 4.3 (**d**, **e**, **f**) of surface water. Filled triangles represent negative acid capacities up to pH 4.3 and empty triangles represent positive acid capacities up to pH 4.3 (based on LMBV mbH 2019, own data)

3.0 to 4.5 with acid capacities up to pH 4.3 from − 6 up to 2 mmol/L are primarily observed in summer. The acid binding capacity decreases with wetland's input. The base capacity up to pH 8.2 is not pH-dependent, but it has decreased over the last years in the whole investigation area (Online Resource 2).

While the total iron concentration, predominating ferrous iron, varies between 200 and 250 mg/L in groundwater, it decreases in surface water downstream from 200 to 100 mg/L (Fig. 3). The sampling locations in the wetland show maximal total iron concentrations of 250 mg/L. Higher undissolved iron amounts at LaF 40 (Online Resource 2) and lower total iron concentrations at LaF 20 than at LaF 30, representing the tributary from the wetland, are observed. The total iron concentration of the surface water is less in summer than in winter. The sulfate concentration in groundwater south of the wetland is around 500 mg/L, while it varies between 1000 and 1500 mg/L in surface water without any spatial dependencies from 2009 to 2019. In contrast to the total iron concentration, a weak increase of the sulfate concentration is detected in surface water in summer. The iron–sulfate ratio of surface water significantly exceeds the value of 1:2. Sulfate and total iron concentration have weakly decreased in groundwater and surface water over the last years (Online Resource 2). The iron loads correlate with the discharge rates: winter loads between 60 and 120 kg/d and summer loads up to 50 kg/d are observed in the upper stream (Fig. 3). The downstream of the drainage stream shows iron loads between 0 kg/d in summer and 200 kg/d in winter.

As can be seen from the plots and the E_H–pH diagrams for the Fe–S–K–O–H system (Fig. 4, Online Resource 2), all waters are moving along the stability lines of schwertmannite and goethite as well as ferrihydrite and goethite, indicating a dynamic iron transformation with a predominance of precipitated ferric iron. While the surface water is dominated by ferrihydrite in the upper stream, LaF 30 and the downstream are characterized by the variation of dominant schwertmannite in summer and ferrihydrite in

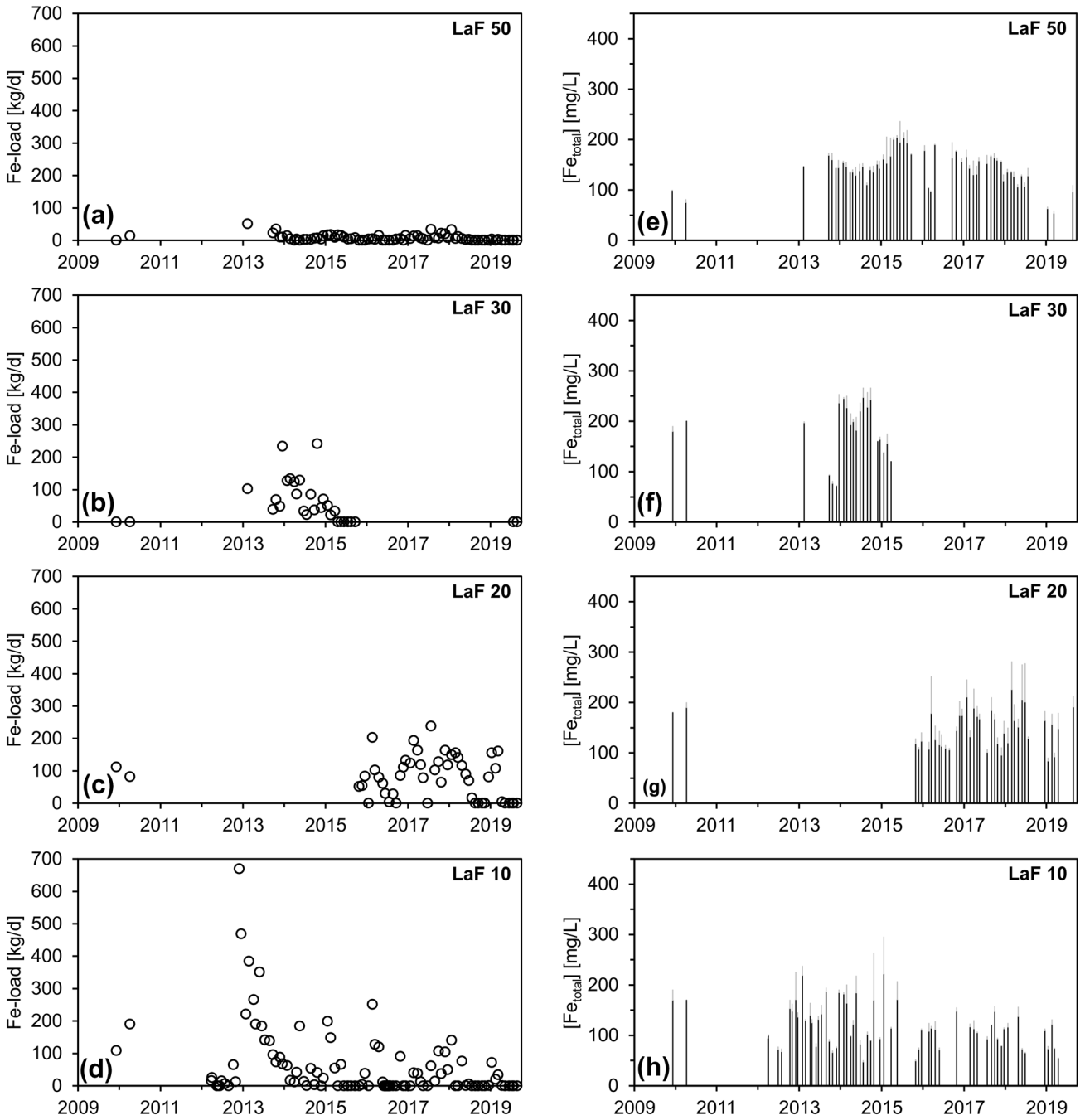

Fig. 3 Time series of iron loads (**a**, **b**, **c**, **d**) and total iron concentrations (**e**, **f**, **g**, **h**) of surface water. Grey bars represent total undissolved iron concentrations, while black bars represent total dissolved iron concentrations (based on LMBV mbH 2019, own data)

winter due to seasonal changes in pH and E_H. In summer, pH varies between 2.8 and 4.1 along schwertmannite's stability field downstream. The determined predominance of precipitated ferric iron in groundwater is not assumed because of measured anoxic conditions. The downstream of the catchment area is dominated by ferric iron, goethite, and schwertmannite due to acidic conditions.

Discussion

Source of iron and sulfate

The highest concentrations of ferrous iron were detected in the surface water in the area of the wetland, indicating a significant output of ferrous iron from the wetland into surface

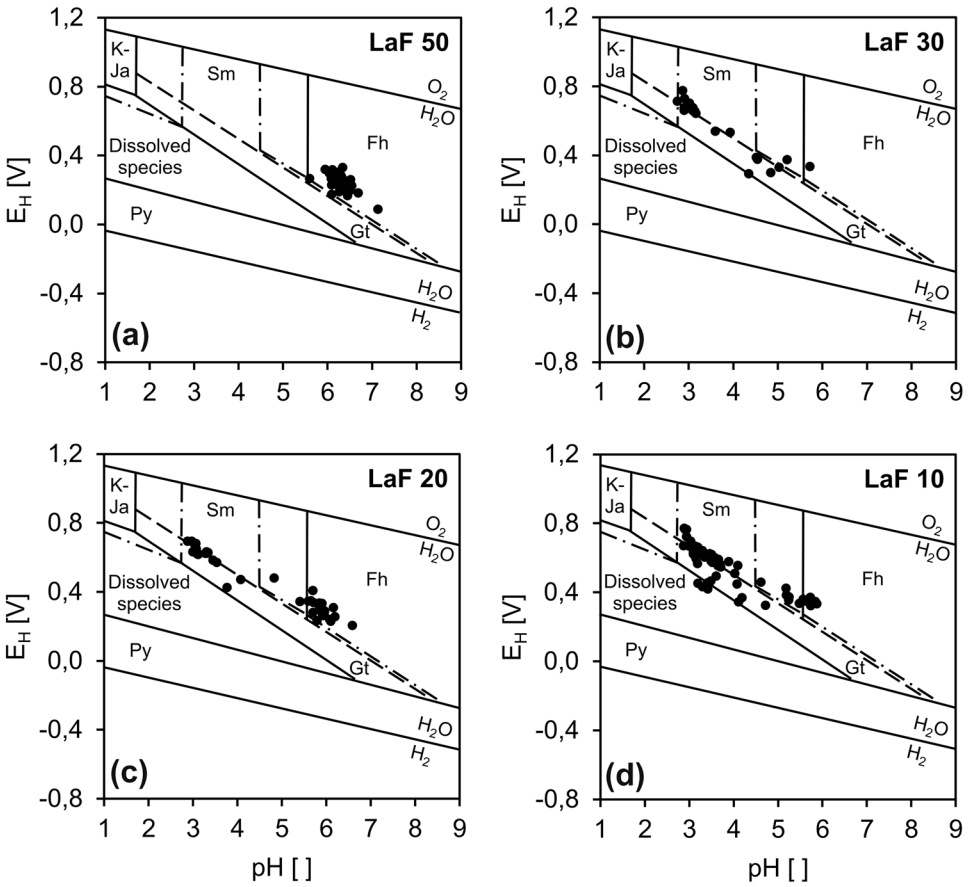

Fig. 4 E_H–pH diagram for the Fe–S–K–O–H system at 25 °C, plotted with long-term data of surface water from 12/09 to 08/19. Stability fields have been adapted from Bigham et al. (1996). K-Ja… K-jarosite, Sm… schwertmannite, Fh… ferrihydrite, Gt…goethite, Py… pyrite. The dashed lines show the metastability field, and the dotted dash lines represent the expanded stability fields of K-jarosite and ferrihydrite depending on sulfate concentrations, etc. (Bigham et al. 1996, based on LMBV mbH 2019, own data)

water. Simultaneously lower concentrations of undissolved iron in the tributary from the wetland (LaF 30) than in LaF 40 show a less progressed iron oxidation in the tributary and thus a proximity to the iron source, located in the wetland.

A current output of weathered pyrite from the water saturated zone of the wetland is not assumed, because there are no pyrite deposits in the peat (Uhlmann et al. 2010) due to aerobic conditions induced by the past groundwater drawdown (Schmidt 2013) and progressing peat degradation. It is also assumed that the high iron concentrations of the surface water are not generated by the dissolution of bog iron ore that still makes up 2.0–4.5 w% of the peat (Uhlmann et al. 2010): first, the lime-free peat (Uhlmann et al. 2010) had accelerated iron leaching in the recent past (Kruspe et al. 2014) due to oxidation, and second, the surface water should be more dominated by ferric iron than ferrous iron.

With respect to the hydrochemical similarity between groundwater and surface water, an origin from groundwater is assumed. Through weathering processes of local pyrite deposits, iron and sulfate were mobilized in the groundwater. The stoichiometric iron–sulfate ratio of 1:2 expected for pyrite weathering is predominantly exceeded in the surface catchment area because of progressing precipitation of ferric iron at pH greater than 4 (Wisotzky 1996). It is assumed that a minor part of the sulfate concentration is generated by weathering and mineralization of organic matter of the peat, being pronounced in summer. This is supported by weakly increasing sulfate concentrations in the surface water of the wetland in summer and by the fact that about 80 w% of the total sulfur of the peat is organically bound (Uhlmann et al. 2010).

Hydrology of the output of iron and sulfate

The absence of baseflow in the surface water while higher groundwater potential in summer indicates groundwater is prevented from infiltrating into the wetland in summer. Due to its low hydraulic conductivity (Schälchli 1992), ferric mud, sedimented as a colmation layer on the riverbed and riverbank of the surface water, acts as an aquitard. It is not assumed that the hydraulic gradient is sufficient for a significant increase of hydraulic conductivity (Rosenberry and Pitlick 2009).

Consequently, iron- and sulfate-rich groundwater is discharged via the wetland to the surface water. Based on

the water table contour map, water-level measurements in winter, and observed signs of desiccation on wetland's surface in summer, the hydraulic connection to groundwater is inhibited. Because there is no mudde layer that underlies the peat (Uhlmann et al. 2010; Landesvermessung und Geobasisinformation Brandenburg 2022), a decreased hydraulic conductivity of the peat, induced by peat degradation (Liu and Lennartz 2019), is assumed. Flow is assumed to be so slow that adhesive forces (Busch et al. 1993) lead to storage of groundwater, loaded with iron and sulfate, in the wetland rather than being transported to the surface water.

The output of iron and sulfate into surface water is controlled by the seasonal varying rates of precipitation, indicated by correlations of climatic water balances, discharge rates, and iron loads. In contrast, diffuse groundwater infiltration plays a minor role in regulating iron loads of the surface water (Kruspe et al. 2014). As a result of the negative climatic water balance and less wet periods in summer, iron and sulfate, fed with the groundwater and stored in the wetland, are retarded in the wetland. In contrast, in winter positive climatic water balances and the trend to wet periods generate dominant supply by infiltrated precipitation, resulting in the strong release of iron and sulfate from the wetland by drainage.

Consequently, the wetland acts recently more like a rain bog than a fen, as the local original wetlands were classified in the past (Uhlmann et al. 2010; Krümmelbein et al. 2012). Because the drained wetland is not constantly fed by groundwater, especially in summer, constant water saturated conditions throughout the year are not ensured. This leads to advanced peat degradation, resulting in loss of the natural water storage filter and buffer capacity (Lamers et al. 2015; Liu et al. 2017).

Transformation processes in the source area and LaF

Iron and sulfate are mainly transformed under aerobic conditions in the wetland and surface water, strongly controlled by seasonal variations in discharge rates and redox conditions. Due to its dominant occurrence in the investigation area and its metastability, schwertmannite gains high relevance in controlling the redox conditions by its buffer function (Regenspurg 2002).

Especially in summer under aerobic conditions while low discharge rates, high retention times (Skousen et al. 2000; Kruspe et al. 2014), and high T and light intensity (Kruspe et al. 2014), iron is oxidized, hydrolysed, and precipitated and thus physically removed from the water phase (Skousen et al. 2000). This is indicated by lower dissolved iron concentrations in summer and decreasing concentrations in surface water along greater distance to the wetland. Due to low acid capacity up to pH 4.3 of wetland's groundwater, the surface water tends to acidify (Fig. 4), enhanced by aerobic oxidation reactions (Lamers et al. 1998). However, pH values below 2.5 would dissolve schwertmannite by bacterial ferric reduction (Peine et al. 2000; Küsel 2003). The resulting release of hydroxide leads to increasing pH (Regenspurg 2002). Neutralisation above pH 4.5 is prevented by re-oxidation and precipitation of schwertmannite (Küsel 2003), provided that a constant supply of ferrous iron is observed (Regenspurg 2002). Thus, removal of major and trace elements like iron keeps up (Bigham et al. 1990, 1996; Regenspurg 2002; Burton et al. 2021) in the wetland and especially downstream (Fig. 3), representing a potential iron sink. Higher wetland's removal ability, while lower source strength and discharge rates were also observed by August et al. (2002).

Negative ion balances and expected positive surface charge of schwertmannite and goethite under acid conditions (Bigham et al. 1996) enable a potential capacity for anion exchange on organic matter and precipitated ferric minerals. However, weakly increasing sulfate concentrations indicate that ferric iron precipitation is not sufficient for a significant removal of sulfur in contrast to iron. The oxidized and acidic conditions on the interface between schwertmannite and water phase also prevent sulfur removal by sulfate reducing bacteria (Peine et al. 2000). Instead, in summer, the wetland tends more to desiccation resulting in aerobic oxidation that leads to mineralization of carbon, subsequent loss of carbon into the atmosphere (Lamers et al. 2015), and loss of DOC and particular carbon (Freeman et al. 2001), which was observed by high DOC concentrations up to 56 mg/l in surface water in the area of the wetland. The summerly oxidation of organic and mineral bound sulfur results in higher sulfate concentrations (Lamers et al. 1998) in the surface water. Evidence for an increased discharge of mineralized nitrogen and phosphorus was not found. While the significant ammonium formation in the surface water is generated by live-stock farming, negligible phosphate concentrations, also confirmed by Uhlmann et al. (2010), can be due to sorption onto ferric precipitations and subordinated aluminium and manganese precipitations (Litaor et al. 2004), plant uptake (Messer et al. 2021), or low background concentrations in the peat.

In contrast, in winter, greater water availability results in higher discharge rates and thus also higher supply of iron and sulfate in the surface water (Fig. 3, Online Resource 2). The greater concentrations in the surface water are generated by leaching (Nordstrom 2009) of stored iron and sulfate in wetland–the wetland acts as a source in winter. There is no dilution effect indicated by precipitation water in the surface water, because the iron and sulfate supply is just being initiated by infiltrated precipitation water. In contrast to summer, the source strength is higher than the removal capacity,

because the retention time, T, and light climatic (Kruspe et al. 2014) are not strong enough to oxidize and precipitate the immense supply of iron and sulfate. The varying high discharge rates generate changing ferrous concentrations, overlaying the concentrations only induced by oxidation. The attenuated oxidation progress leads to higher pH and more predominant saturation of the proximal surface water with ferrihydrite and goethite than with schwertmannite in winter. Increased sulfate concentrations that can be generated by lower sulfate adsorption capacity of ferrihydrite and goethite than schwertmannite's sulfate bonding capacity (Bigham et al. 1996) were not observed.

Even though evidence of wetland's retention potential, especially in summer by iron oxidation and precipitation, was found, it is strongly weakened to almost non-existent by progressing peat degradation in summer and high source strength in winter.

Conclusions and outlook

The high iron and sulfate concentrations in surface water dominantly originate from groundwater, temporally stored in the wetland. Due to long-term drainage, the wetland's hydraulic connection to groundwater is inhibited, leading to a stronger dependence of the water supply on seasonal varying infiltrated precipitation water, which is maximal in winter. In summer, under aerobic conditions, peat degradation is progressing, resulting in transformation, dissolution, and loss of organic matter and its bound components. While the wetland acts as a sink in summer due to progressed iron oxidation and weak water supply, greater water supply induces a high source strength of iron and sulfate in winter, being discharged by the drainage via the surface water. Schwertmannite's significant role in pH-buffering and subordinately iron removal could be demonstrated.

Because Lusatia is expected to be exposed to longer drought periods in summer and increasing water-deficient years (Pohle et al. 2012), leading to locally decreased groundwater recharge (Lorenz 2008), wetland's natural buffer function is going to increasingly weaken, while winter months gain higher relevance in output. However, the weakly decreasing concentrations of iron and sulfate in the catchment area in the last few years indicate an attenuated source strength that lead to further lower output rates.

This study demonstrates wetlands' significantly altered effect on matter transformation, retention, and output, generated by hydrological and hydrochemical changes due to long-term anthropogenic influence on local water balance. As a consequence, Briesener Niedermoor is not able to protect the surface water from AMD. However, rewetting of the wetland by terminating drainage may increase the peat thickness and thus the retention capability.

Supplementary Information The online version contains supplementary material available at https://doi.org/10.1007/s12665-023-10751-3.

Acknowledgements The authors would like to thank Lausitzer und Mitteldeutsche Bergbau-Verwaltungsgesellschaft mbH (LMBV mbH) for providing the data and its support. The authors would also like to thank all those who supported the data collection in the lab as well as in the field.

Author contributions All authors contributed to the study conception and design. Material preparation, data collection, and analysis were performed by Clemens Hartmann, Wilfried Uhlmann, and Traugott Scheytt. The first draft of the manuscript was written by Clemens Hartmann and all authors commented on previous versions of the manuscript. All authors read and approved the final manuscript.

Funding Open Access funding enabled and organized by Projekt DEAL. The authors declare that no funds, grants, or other supports were received during the preparation of this manuscript.

Availability of data and materials The data that support the findings of this study are available in the Supplementary Information as Online Resource as well as on request from the corresponding author, Clemens Hartmann.

Declarations

Conflict of interest The authors have no relevant financial or non-financial interests to disclose.

References

August EE, McKnight DM, Hrncir DC, Garhart KS (2002) Seasonal variability of metals transport through a wetland impacted by mine drainage in the Rocky Mountains. Environ Sci Technol 36(17):3779–3786. https://doi.org/10.1021/es015629w

Bayley SE, Behr RS, Kelly CA (1986) Retention and release of S from a freshwater wetland. Water Air Soil Pollut 31:101–114. https://doi.org/10.1007/978-94-009-3385-9_116

Beining B, Otte ML (1996) Retention of metals originating from an abandoned lead Zinc mine by a wetland at Glendalough, Co. Wicklow. Biol Environ 96B(2):117–126

Berghorn GH, Hunzeker GR (2001) Passive treatment alternatives for remediating abandoned-mine drainage. Remediation 11(3):111–127. https://doi.org/10.1002/rem.1007

Bigham JM, Schwertmann U, Carlson L, Murad E (1990) A poorly crystallized oxyhydroxysulfate of iron formed by bacterial oxidation of Fe(II) in acid mine waters. Geochim Cosmochim Acta 54:2743–2758. https://doi.org/10.1016/0016-7037(90)90009-A

Bigham JM, Carlson L, Murad E (1994) Schwertmannite, a new iron oxyhydroxysulphate from Pyhäsalmi, Finland, and other localities. Mineral Mag 58(393):641–648. https://doi.org/10.1180/minmag.1994.058.393.14

Bigham JM, Schwertmann U, Traina SJ, Winland RL, Wolf M (1996) Schwertmannite and the chemical modelling of iron in acid sulfate waters. Geochim Cosmochim Acta 60(12):2111–2121. https://doi.org/10.1016/0016-7037(96)00091-9

Blowes DW, Ptacek CJ, Jambor JL, Weisener CG, Paktunc D, Gould WD, Johnson DB (2014) The geochemistry of acid mine drainage. In: Holland HD, Turekian KK (eds) Treatise on geochemistry, vol 11, 2nd edn. Elsevier, pp 131–190. https://doi.org/10.1016/B978-0-08-095975-7.00905-0

Burton ED, Karimian N, Johnston SG, Schoepfer VA, Choppala G, Lamb D (2021) Arsenic-imposed effects on schwertmannite and jarosite formation in acid mine drainage and coupled impacts on arsenic mobility. ACS Earth Space Chem 5(6):1418–1435. https://doi.org/10.1021/acsearthspacechem.1c00047

Busch KF, Luckner L, Tiemer K (1993) Lehrbuch der Hydrogeologie Band 3: Geohydraulik, 3rd edn. Gebrüder Borntraeger, Berlin, pp 105–107

Carrero S, Pérez-López R, Fernandez-Martinez A, Cruz-Hernández P, Ayora C, Poulain A (2015) The potential role of aluminium hydroxysulphates in the removal of contaminants in acid mine drainage. Chem Geol 417:414–423. https://doi.org/10.1016/j.chemgeo.2015.10.020

Chiang W-H, Kinzelbach W (2001) Processing mudflow. Version 5.3.1. Hamburg, Zürich

Dean AP, Lynch S, Rowland P, Toft BD, Pittman JK, White KN (2013) Natural wetlands are efficient at providing long-term metal remediation of freshwater systems polluted by acid mine drainage. Environ Sci Technol 47(21):12029–12036. https://doi.org/10.1021/es4025904

Devito KJ, Hill AR (1997) Sulphate dynamics in relation to groundwater-surface water interactions in headwater wetlands of the southern canadian shield. Hydrol Process 11(5):485–500. https://doi.org/10.1002/(SICI)1099-1085(199704)11:5%3c485::AID-HYP455%3e3.0.CO;2-F

Dos Santos EC, de Mendonça Silva JC, Duarte HA (2016) Pyrite oxidation mechanism by oxygen in aqueous medium. J Phys Chem C 120(5):2760–2768. https://doi.org/10.1021/acs.jpcc.5b10949

Eimers S, Catherine M, Watmough SA, Buttle JM, Dillon PJS (2008) Examination of the potential relationship between droughts, sulphate and dissolved organic carbon at a wetland-draining stream. Glob Change Biol 14(4):938–948. https://doi.org/10.1111/j.1365-2486.2007.01530.x

Freeman C, Evans CD, Monteith DT (2001) Export of organic carbon from peat soils. Nature 412:785. https://doi.org/10.1038/35090628

Galhardi JA, Bonotto DM (2016) Hydrogeochemical features of surface water and groundwater contaminated with acid mine drainage (AMD) in coal mining areas: a case study in southern Brazil. Environ Sci Pollut Res 23(18):18911–18927. https://doi.org/10.1007/s11356-016-7077-3

Humphries MS, McCarthy TS, Pillay L (2017) Attenuation of pollution arising from acid mine drainage by a natural wetland on the Witwatersrand. S Afr J Sci. https://doi.org/10.17159/sajs.2017/20160237

Ighalo JO, Kurniawan SB, Iwuozor KO, Aniagor CO, Ajala OJ, Oba SN, Iwuchukwu FU, Ahmadi S, Igwegbe CA (2022) A review of treatment technologies for the mitigation of the toxic environmental effects of acid mine drainage (AMD). Process Saf Environ Prot 157:37–58. https://doi.org/10.1016/j.psep.2021.11.008

Knorr K-H, Blodau C (2007) Controls on schwertmannite transformation rates and products. Appl Geochem 22(9):2006–2015. https://doi.org/10.1016/j.apgeochem.2007.04.017

Krümmelbein J, Bens O, Raab T, Naeth MA (2012) A history of lignite coal mining and reclamation practices in Lusatia, eastern Germany. Can J Soil Sci 92(1):53–66. https://doi.org/10.4141/cjss2010-063

Kruspe R, Neumann J, Opitz M, Theiss S, Uhlmann W, Zimmermann K (2014) Fließgewässerorganismen und Eisen: Qualitative und quantitative Beeinflussungen von Fließgewässerorganismen durch Eisen am Beispiel der Lausitzer Braunkohlefolgelandschaft. Schriftenreihe des LfULG 2014(35)

Küsel K (2003) Microbial cycling of iron and sulfur in acidic coal mining lake sediments. Water Air Soil Pollut 3:67–90. https://doi.org/10.1023/A:1022103419928

Lamers LPM, van Roozendaal SME, Roelofs JGM (1998) Acidification of freshwater wetlands: combined effects of non-airborne sulfur pollution and desiccation. Water Air Soil Pollut 105:95–196. https://doi.org/10.1023/A:1005083526455

Lamers LPM, Vile MA, Grootjans AP, Acreman MC, van Diggelen R, Evans MG, Richardson CJ, Rochefort L, Kooijman AM, Roelofs JGM, Smolders AJP (2015) Ecological restoration of rich fens in Europe and North America: from trial and error to an evidence-based approach. Biol Rev Camb Philos Soc 90:182–203. https://doi.org/10.1111/brv.12102

Landesvermessung und Geobasisinformation Brandenburg (2022) Geologische Karte des Landes Brandenburg. https://geoportal.brandenburg.de/de/cms/portal/start/map/34. Accessed 10 Mar 2022

Landgraf L (2010) Wo steht der Moorschutz in Brandenburg? Naturschutz und Landschaftspflege in Brandenburg: Beiträge zu Ökologie, Natur- und Gewässerschutz 19 (34):126–131

Litaor MI, Reichmann O, Auerswald K, Haim A, Shenker M (2004) The geochemistry of phosphorus in peat soils of a semiarid altered wetland. Soil Sci Soc Am J 68(6):2078–2085. https://doi.org/10.2136/sssaj2004.2078

Liu H, Lennartz B (2019) Hydraulic properties of peat soils along a bulk density gradient—a meta study. Hydrol Process 33(1):101–114. https://doi.org/10.1002/hyp.13314

Liu H, Forsmann DM, Kjærgaard C, Saki H, Lennartz B (2017) Solute transport properties of fen peat differing in organic matter content. J Environ Qual 46(5):1106–1113. https://doi.org/10.2134/jeq2017.01.0031

Lorenz M (2008) Auswirkungen von Klimaveränderungen auf Bodenwasserhaushalt, Biomasseproduktion und Degradierung von Niedermooren im Spreewald. Ph. D. Thesis, TU Berlin

McCarthy TS, Arnold V, Venter J, Ellery WN (2016) The collapse of Johannesburg's River wetland. S Afr J Sci 103:391–397. https://doi.org/10.5194/gi-2016-11-RC2

Messer TL, Moore TL, Nelson N, Ahiablame L, Bean EZ, Boles C, Cook SL, Hall SG, McMaine J, Schlea D (2021) Constructed wetlands for water quality improvement: a synthesis on nutrient reduction from agricultural effluents. Trans ASABE 64(2):625–639. https://doi.org/10.13031/trans.13976

Moreno-González R, Macías F, Olías M, Ruiz Cánovas C (2022) Temporal evolution of acid mine drainage (AMD) leachates from the abandoned tharsis mine (Iberian Pyrite Belt, Spain). Environ Pollut 295:118697. https://doi.org/10.1016/j.envpol.2021.118697

Moreno-Mateos D, Comin FA (2010) Integrating objectives and scales for planning and implementing wetland restoration and creation in agricultural landscapes. J Environ Manage 91(11):2087–2095. https://doi.org/10.1016/j.jenvman.2010.06.002

Moses CO, Nordstrom DK, Herman JS, Mills AL (1987) Aqueous pyrite oxidation by dissolved oxygen and by ferric iron. Geochim Cosmochim Acta 51(6):1561–1571. https://doi.org/10.1016/0016-7037(87)90337-1

Nordstrom DK (2009) Acid rock drainage and climate change. J Geochem Explor 100(2–3):97–104. https://doi.org/10.1016/j.gexplo.2008.08.002

Nordstrom DK, Blowes DW, Ptacek CJ (2015) Hydrogeochemistry and microbiology of mine drainage: an update. Appl Geochem 57:3–16. https://doi.org/10.1016/j.apgeochem.2015.02.008

Nordstrom DK (1982) Aqueous Pyrite Oxidation and the Consequent Formation of Secondary Iron Minerals. In: Kittrick JA, Fanning DS, Hossner LR (ed) Acid Sulfate Weathering, Soil Science Society of America, Madison, WI, USA, 37–56. https://doi.org/10.2136/sssaspecpub10.c3

Pat-Espadas A, Loredo Portales R, Amabilis-Sosa L, Gómez G, Vidal G (2018) Review of constructed wetlands for acid mine drainage treatment. Water 10(11):1685. https://doi.org/10.3390/w10111685

Peine A, Tritschler A, Küsel K, Peiffer S (2000) Electron flow in an iron-rich acidic sediment-evidence for an acidity-driven iron cycle. Limnol Oceanogr 45(5):1077–1087. https://doi.org/10.4319/lo.2000.45.5.1077

Pohle I, Koch H, Grünewald U (2012) Potential climate change impacts on the water balance of subcatchments of the River Spree, Germany. Adv Geosci 32:49–53. https://doi.org/10.5194/adgeo-32-49-2012

Regenspurg S (2002) Characterisation of Schwertmannite: Geochemical Interactions with Arsenate and Chromate and Significance in Sediments of Lignite Opencast Lakes. Ph. D. Thesis, Universität Bayreuth

Rosenberry DO, Pitlick J (2009) Effects of sediment transport and seepage direction on hydraulic properties at the sediment–water interface of hyporheic settings. J Hydrol 373(3–4):378. https://doi.org/10.1016/j.jhydrol.2009.04.030

Sáinz A, Grande JA, de La Torre ML, Sánchez-Rodas D (2002) Characterisation of sequential leachate discharges of mining waste rock dumps in the Tinto and Odiel rivers. J Environ Manage 64(4):345–353. https://doi.org/10.1006/jema.2001.0497

Sasaki K (1994) Effect of grinding on the rate of oxidation of pyrite by oxygen in acid solutions. Geochim Cosmochim Acta 58(21):4649–4655. https://doi.org/10.1016/0016-7037(94)90197-X

Sasaki K, Ogino T, Endo Y, Kurosawa K (2001) Field study on heavy metal accumulation in a natural wetland receiving acid mine drainage. Mater Trans 42(9):1877–1884. https://doi.org/10.2320/matertrans.42.1877

Schälchli U (1992) The clogging of coarse gravel river beds by fine sediment. Hydrobiologia 235(236):189–197. https://doi.org/10.1007/BF00026211

Schmidt A (2013) Inventarisierung sowie genetisch, pedologische und geochemische Kennzeichnung der Niedermoore in den von der Grundwasserabsenkung betroffenen Gebieten im Nordraum der LMBV. Thesis, TU Dresden

Schöpke R (2007) Vergleich der Aufbereitungsleistungen verschiedener aktiver, passiver und in-situ Verfahren zur Behandlung bergbauversauerter Wässer (AMD). In: TU Bergakademie Freiberg (ed) Behandlungstechnologien für bergbaubeeinflusste Wässer, GIS - Geowissenschaftliche Anwendungen und Entwicklungen. With assistance of Merkel BJ, Schaeben H, Hasche-Berger A, Wolkersdorfer C, 58. Berg- und Hüttenmännischer Tag, Freiberg, 14 -15 May 2007, 57–61

Schwertmann U (1991) Solubility and dissolution of iron oxides. Plant Soil 130:1–25. https://doi.org/10.1007/BF00011851

Sekarjannah FA, Wardoyo SS, Ratih YW (2019) Management of mine acid drainage in a constructed wetland using hyacinth plant and addition of organic materials. J Degrade Min Land Manage 6(4):1847–1855. https://doi.org/10.15243/jdmlm.2019.064.1847

Sheoran AS, Sheoran V (2006) Heavy metal removal mechanism of acid mine drainage in wetlands: a critical review. Miner Eng 19(2):105–116. https://doi.org/10.1016/j.mineng.2005.08.006

Sheridan G, Harding K, Koller E, de Pretto A (2013) A comparison of charcoal- and slag-based constructed wetlands for acid mine drainage remediation. Water SA. https://doi.org/10.4314/wsa.v39i3.4

Skousen JG, Zipper CE, Rose A, Ziemkiewicz PF, Nairn R, McDonald LM, Kleinmann RL (2017) Review of passive systems for acid mine drainage treatment. Mine Water Environ 36(1):133–153. https://doi.org/10.1007/s10230-016-0417-1

Skousen JG, Sexstone A, Ziemkiewicz PF (2000) Acid Mine Drainage Control and Treatment. In: Barnhisel RI, Darmody RG, Lee DW (ed) Reclamation of Drastically Disturbed Lands, American Society of Agronomy, Crop Science Society of America, Soil Science Society of America, Madison, WI, USA, 1–42. https://doi.org/10.2134/agronmonogr41.c6

Tutu H, McCarthy TS, Cukrowska E (2008) The chemical characteristics of acid mine drainage with particular reference to sources, distribution and remediation: the Witwatersrand Basin, South Africa as a case study. Appl Geochem 23(12):3666–3684. https://doi.org/10.1016/j.apgeochem.2008.09.002

Uhlmann W, Seiler D, Zimmermann K, Theiss S, Engelmann C, Lommatzsch P (2010) Studie zu den Auswirkungen des Grundwasseranstiegs auf die Beschaffenheit der Oberflächengewässer in den Sanierungsgebieten B1 (Seese/Schabendorf) und B2 (Greifenhain/Gräbendorf): Abschlussbericht Dezember 2010, IWB Dresden, Dresden

Uhlmann W, Theiss S, Nestler W, Claus T (2013) Studie zu den Auswirkungen des Grundwasserwiederanstiegs auf die Beschaffenheit der Oberflächengewässer in den Sanierungsgebieten B1 (Seese/Schlabendorf) und B2 (Greifenhain/Gräbendorf): Projektphase 2: Vertiefung der Untersuchungen zur Präzisierung der Modellgrundlagen und der Bemessungsansätze für Wasserbehandlungsanlagen, IWB Dresden, Dresden

USGS (2020) PHREEQC interactive. Version 3.6.2.15100. USGS, Denver

Deutscher Wetterdienst (2021) CDC-Portal. Deutscher Wetterdienst. https://opendata.dwd.de/climate_environment/CDC/observations_germany/climate/. Accessed 8 Sep 2021

Wiersma CL, Rimstidt JD (1983) Rates of reaction of pyrite and marcasite with ferric iron at pH 2. Geochim Cosmochim Acta 48:85–92. https://doi.org/10.1016/0016-7037(84)90351-X

Wisotzky F (1996) Hydrogeochemische Reaktionen im Sicker- und Grundwasserbereich von Braunkohlentagebaukippen. Grundwasser 3–4:129–136. https://doi.org/10.1007/s767-1996-8480-1

Wolkersdorfer C, Bowell R (2004) Contemporary reviews of mine water studies in Europe, Part 1. Mine Water Environ 23(4):162–182. https://doi.org/10.1007/s10230-004-0060-0

Zubair A, Abdullah NO, Ibrahim R, Rachma ARD (2020) Effectivity of constructed wetland using Typha angustifolia in analyzing the decrease of heavy metal (Fe) in acid mine drainage. IOP Conf Ser 419(012160):1–6. https://doi.org/10.1088/1755-1315/419/1/012160